Computational and Theoretical Chemistry 1130 (2018) 33–45

Contents lists available at ScienceDirect

Computational and Theoretical Chemistry

journal homepage: www.elsevier.com/locate/comptc

Electronic structure of phosphorene nanoflakes. A theoretical insight

Esaú Martínez Olmeda, Cesar Gabriel Vera, Serguei Fomine *

Instituto de Investigaciones en Materiales, Universidad Nacional Autónoma de México, Apartado Postal 70-360, CU, Coyoacán, México DF 04510, Mexico

ARTICLE INFO

Article history:
Received 14 December 2017
Received in revised form 14 February 2018
Accepted 9 March 2018
Available online 10 March 2018

Keywords:
Phosphorene
Nanoflake
Hybrid functional
Relaxation energies
Ionization potential
Electron affinity

ABSTRACT

Phosphorene nanoflakes of different shapes and sizes were studied at the hybrid BHandHLYP level of theory. This functional accurately reproduces the experimental bond lengths and valence angles of black phosphorus. All nanoflakes were found to have a singlet ground state and their band gaps (E_gs) decrease linearly with 1/N, where N is the number of P atoms in the nanoflakes. It seems that the topology of the nanoflake edges does not affect E_g. The ionization potentials (IPs) and electron affinities (EAs) generally grow smaller with increasing nanoflake size. The change in IPs and EAs with size correlate with the delocalization pattern of polaron cations and anions. The shape and nature or the longest edge (zig-zag or armchair) affect both the IP and EA. Nanoflakes with a long zigzag edge have higher IPs and lower EAs compared to square systems. Low theoretically calculated hole reorganization energies (less than 0.1 eV) are in agreement with the experimentally determined high hole mobility in phosphorene. The low hole reorganization energies are due to the better ability of phosphorene nanoflakes to delocalize polaron cations compared to polaron anions.

1. Introduction

Black phosphorus (BP), an allotropy of phosphorus, was discovered more than a century ago [1]. The BP structure is similar to that of graphite, consisting of layers united by dispersion forces [2]. Similarly to graphene, a single layer of graphite, which was prepared by mechanical exfoliation in 2004, a single layer of BP was successfully exfoliated from bulk BP ten years after that, in 2014 [3]. A single layer of BP is called phosphorene, in similitude with graphene. However, phosphorene is different from graphene in many aspects. Graphene has a completely planar structure consisting of fused benzene rings, with no band gap (E_g) and a semimetal nature [4]. Conversely, phosphorene is not planar. It has a puckered structure, as shown in Fig. 1.

Unlike graphene, the properties of phosphorene are strongly anisotropic. Thus, the conductance of phosphorene is up to 50% higher in the armchair than in the zigzag direction [3]. Many of the properties of phosphorene can be modified by applying strain to the material [5]. The most recent experimental data show that phosphorene in a bilayer is a semiconductor with a E_g of 1.88 ± 0.24 eV [6]. The band gap of phosphorene can be modified by applying strain [7].

Since graphene has a band gap of zero, its application in electronic devices is restricted. Graphene nanoribbons and nanoflakes, however, have a finite band gap. The electron confinement and the effect of the edges open up a band gap that depends on the size of the nanoribbon or the nanoflake. Although phosphorene itself has a finite band gap, phosphorene nanoflakes are unique objects from both experimental and theoretical points of view.

Most of the theoretical work on phosphorene has been conducted using periodic boundary conditions models (PBC) [8–13]. Normally, PBC models use pure functionals that suffer from the self-interaction error [14], resulting in overestimated bond lengths and overdelocalization problems. Moreover, some of the important characteristics of the material related to the charge mobility, like reorganization energies, can only be obtained using finite models. PBC models have been applied to study both phosphorene itself and phosphorene nanoribbons.

Phosphorene nanoflakes are interesting potential synthetic targets. The electron confinement in a nanoflake affects its electronic properties. Therefore, the electronic properties of a nanoflake can be tailored by the modification of its size and shape. The shape modification of phosphorene is especially interesting due to the strong anisotropy of the phosphorene properties. Another possibility to tailor the electronic properties of phosphorene nanoflakes is the modification of the terminal groups, which is not an option for phosphorene itself. In a very recent work, hydrogen and fluorine passivated square phosphorene nanoflakes were studied using

* Corresponding author.
E-mail address: fomine@unam.mx (S. Fomine).

https://doi.org/10.1016/j.comptc.2018.03.007
2210-271X/

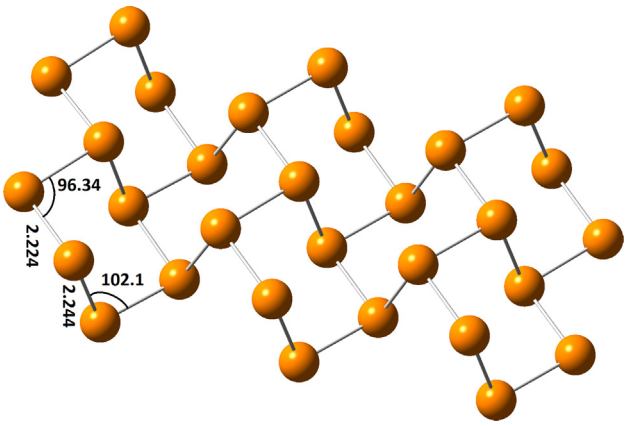

Fig. 1. Experimental bond lengths (Å) and valence angles (degree) geometry in black phosphorus from ref 18.

gradient-corrected functionals. Phosphorene nanoflakes have been proposed as promising materials for solar cells [11].

Therefore, this manuscript provides a detailed study of the electronic properties of phosphorene nanoflakes of different sizes and different shapes.

2. Computational details

All calculations were performed using the TURBOMOLE 7.2 code [15]. Geometry optimizations were carried out using the D3BJ [16] dispersion-corrected BHandHLYP functional [17] in combination with the def2-SVP basis set [18]. All studied nanoflakes are shown in Figs. 2–4. The free valences of edged atoms were saturated with hydrogens. All nanoflakes are denoted as **m** × **n** where **m** is the number of hexagons in the zigzag direction and **n** is the number of hexagons in the armchair direction, (−) or (**+**) represents the anion and cation radicals, respectively.

We tested different functionals using the experimental geometry of BP as a reference [19]. All tested pure or gradient-corrected

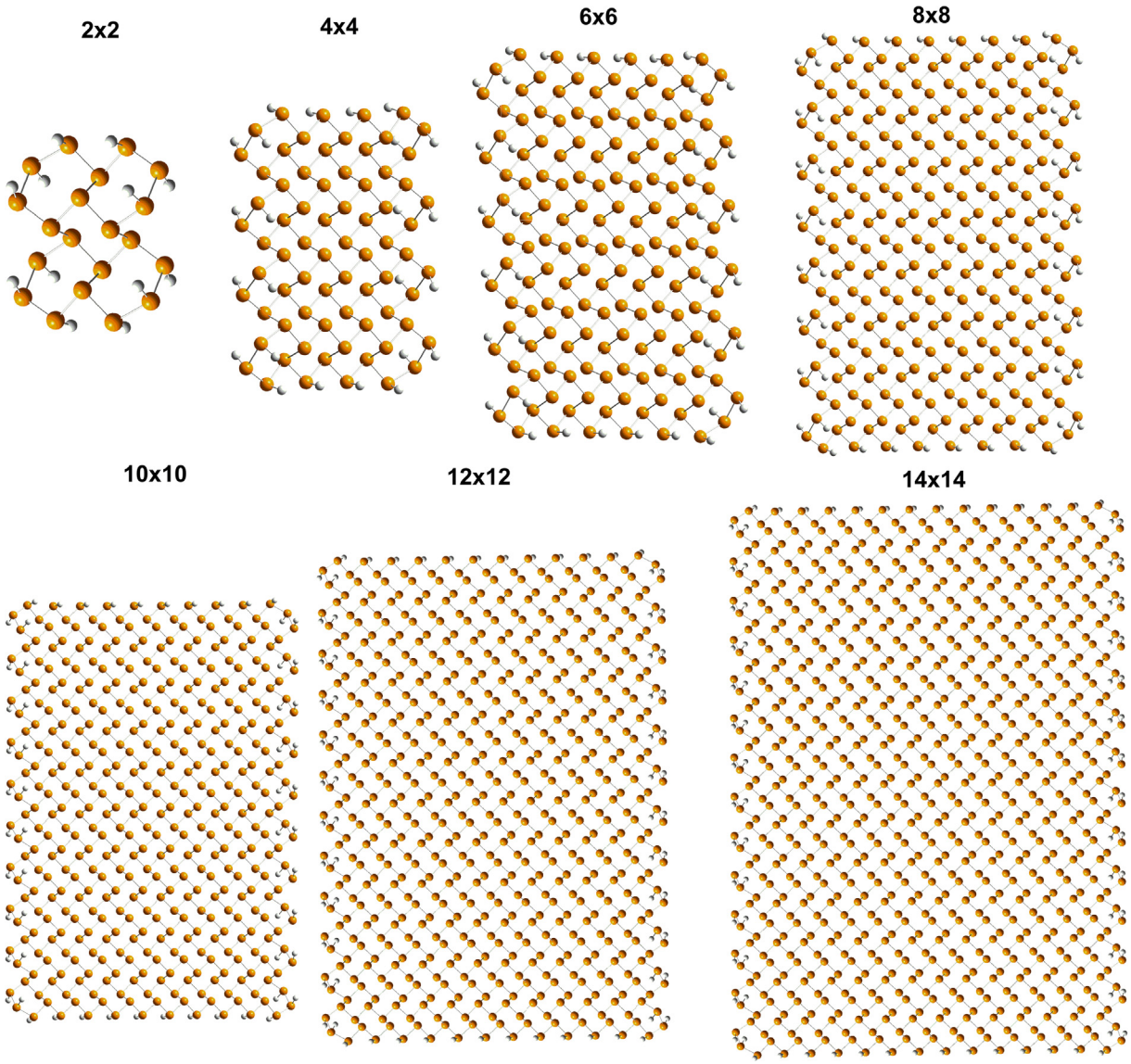

Fig. 2. Optimized structures of **n** × **n** nanoflakes.

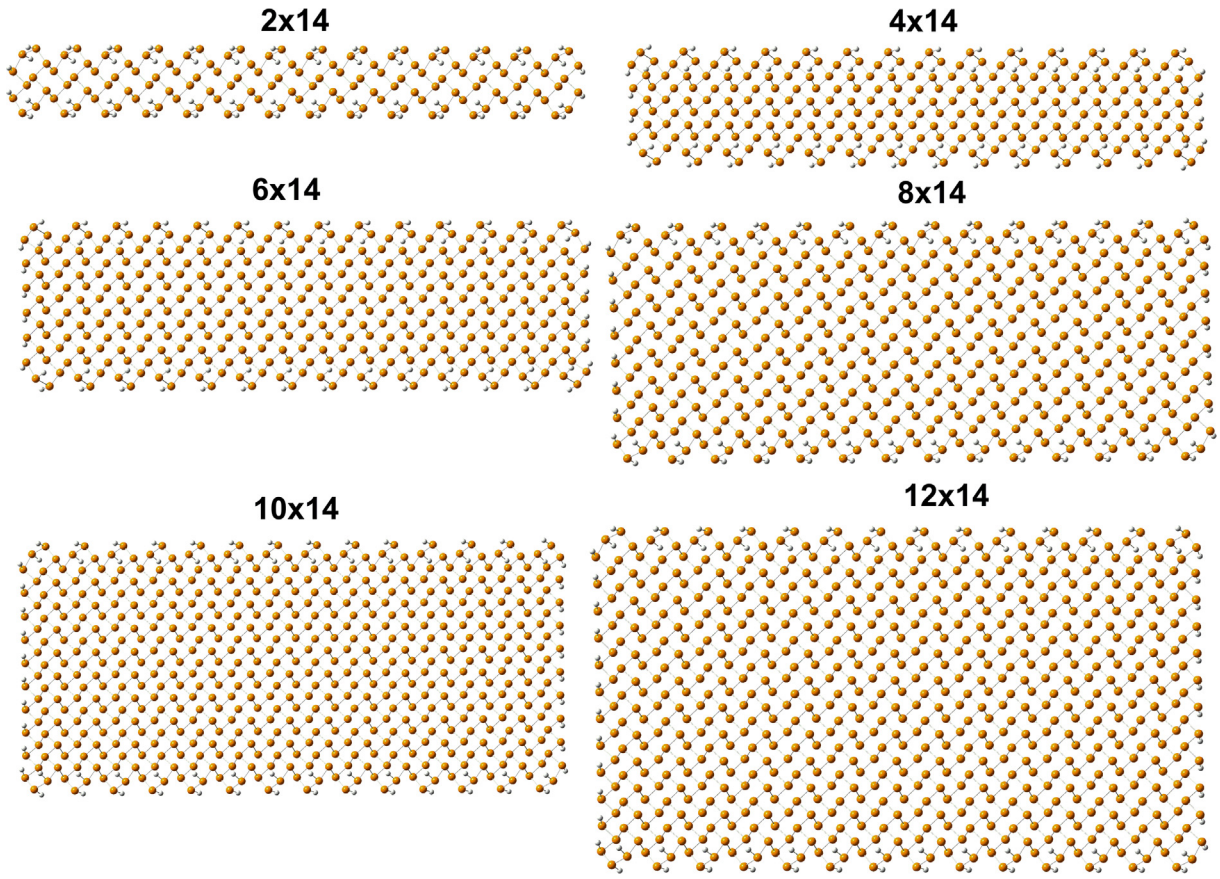

Fig. 3. Optimized structures of **m** × **14** nanoflakes.

functionals overestimated the P-P distances by 0.05–0.07 Å. Hybrid functionals performed better and the best results were delivered by the BHandHLYP functional.

The D3BJ dispersion-corrected BHandHLYP functional in combination with a def2-SVP basis set predicts the bond length of two nonequivalent P-P bonds as 2.242 and 2.212 Å for the central hexagon of the largest studied nanoflake, **14** × **14**, which compares very favorably with the experimentally determined 2.244 and 2.224 Å, respectively, [19], obtained from the X-ray diffraction data of BP. The deviation of the calculated P-P-P angles from those experimentally determined did not exceed 1°.

The structures of the smallest nanoflakes were optimized assuming the C_1 symmetry group. After optimization, all systems adopted C_{2h} symmetry, therefore, all other systems were optimized assuming C2h symmetry.

The band gaps of the nanoflakes were calculated as the S0 → S1 excitation energies using the time dependent (TD) DFT method. Although the band gaps for BP and phosphorene have been determined experimentally, there are no experimental data available for phosphorene nanoflakes. Therefore, we used excitation energies obtained with the approximate second order couple cluster method (CC2) [20], in combination with a large def2-TZVP [18] basis set for the **2** × **2** nanoflake as a reference. The CC2 calculated S0 → S1 excitation energy for the **2** × **2** nanoflake and the experimental E_g of the phosphorene were used to select the functional for TD calculations. The optimum results were obtained for the B3LYP functional. The TD-B3LYP method predicts a E_g of 1.77 eV for the **14** × **14** nanoflake, in good agreement with the experimentally determined band gap for the bilayer of phosphorene of 1.88 eV [6]. Alternatively, the CC2 and TD-B3LYP methods gave S0–S1 excitation energies of 3.30 and 3.25 eV, respectively, for **2** × **2** nanoflakes, in very good agreement with each other. All TD calculations were carried out using the same def2-TZVP basis set, the same basis set applied for the CC2 calculations.

It is crucial to understand factors related with the conductivity of the nanoflakes. It is known that in the solid state, the hole mobility in arylamines is closely related to the internal reorganization energy (λ) [21–23]. One can estimate the hole reorganization energy (λ_+) in systems dominated by local vibronic coupling as follows:

$$\lambda_+ = (E_n^+ - E_n) + (E_+^n - E_+)$$

where E_n and E_+ are the energies of the neutral and cationic species in their lowest energy geometries, respectively, while E_n^+ and E_+^n are the energies of the neutral and cationic species with the geometries of the cation and neutral species, respectively. For electron transport, the reorganization energy can be defined similarly:

$$\lambda_- = (E_n^- - E_n) + (E_-^n - E_-)$$

In this case, E_n and E_- are the energies of the neutral and anion species in their lowest energy geometries, respectively, while E_n^- and E_-^n are the energies of the neutral and anion species with the geometries of the cation and neutral species, respectively.

3. Results and discussion

3.1. Neutral nanoflakes

Figs. 2–4 show the optimized structures of the phosphorene nanoflakes.

Fig. 2 shows nanoflakes of the **n** × **n** series, while Figs. 3 and 4 show nanoflakes of the **m** × **14** and **14** × **n** series, respectively.

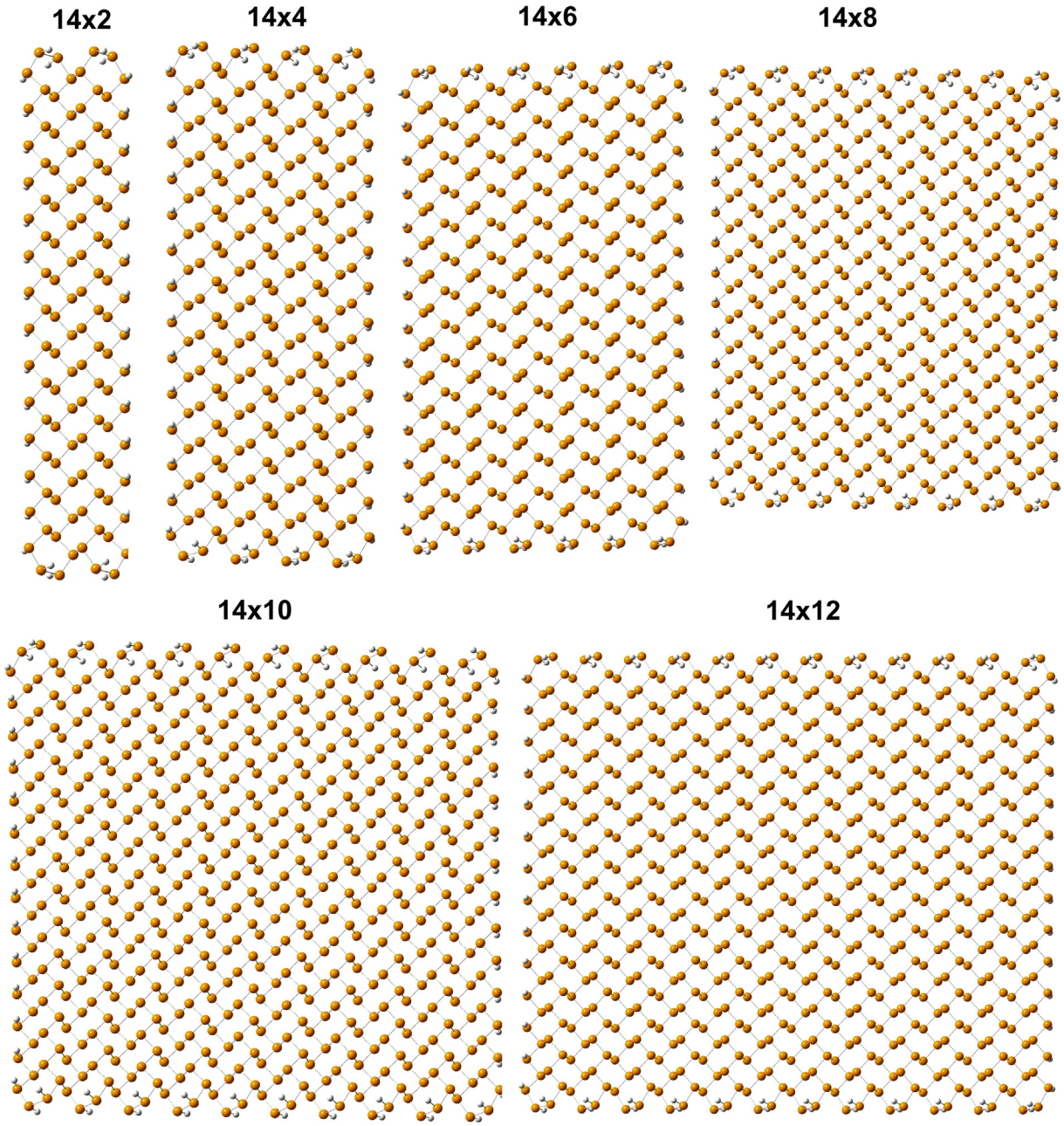

Fig. 4. Optimized structures of **14** × **n** nanoflakes.

Unlike graphene nanoflakes (GNFs), where the nature of the ground state is not necessarily singlet and higher multiplicity ground states are common [24–26], all studied phosphorene nanoflakes have singlet ground states. The optimized geometries of neutral and charged phosphorene nanoflakes are given in the Supporting information.

According to the calculations, the geometries of neutral nanoflakes do no vary significantly with the size or shape of the nanoflake. The bond lengths vary only within 0.01 Å. The only exception is the smallest **2** × **2** nanoflake, where the edge effects are very strong, leading to a shorter bond length by some 0.03 Å, compared to larger systems.

The bond angles vary more. However, they vary not between but within a nanoflake. The difference is most notable for the atoms belonging to the edges. Thus, the zigzag angle in the nanoflakes for the atoms at the juncture between the armchair and zigzag edges rises from 96 to 108°. This effect is similar for all nanoflakes, independent of the size and shape.

Fig. 5 depicts the evolution of E_g in the phosphorene nanoflakes with size and shape. As seen, E_g drops notably with size for all types of the nanoflakes from 3.30 eV for **2** × **2**, approaching 1.8 eV for the largest **14** × **14** nanoflake, very close to the E_g of pure phosphorene. The E_g of the phosphorene nanoflakes depends also on their shape. To explore this effect, we plotted the calculated E_g against the total number of phosphorus atoms in the nanoflake (Fig. 6).

As seen, the E_g is lower for square **n** × **n** nanoflakes compared to **14** × **n** or **m** × **14** ones with similar numbers of atoms. All other things being equal, rectangular nanoflakes have higher E_g compared with square ones. The difference between the E_gs of rectangular and squared nanoflakes decreases with **m** or **n** for **14** × **n** and **m** × **14** systems as the nanoflakes are converged to the **14** × **14**

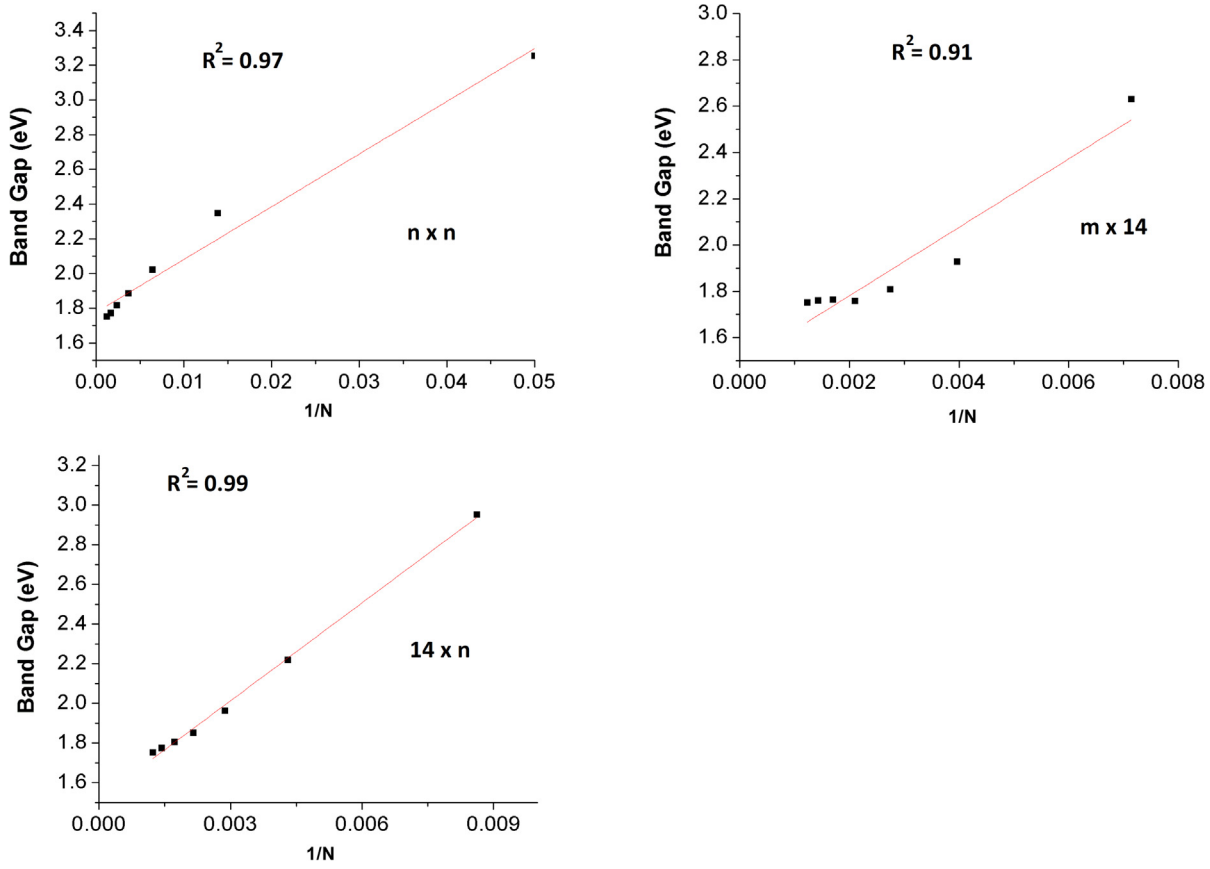

Fig. 5. Evolution of the band gaps with the reciprocal of the number of atoms (**1/N**).

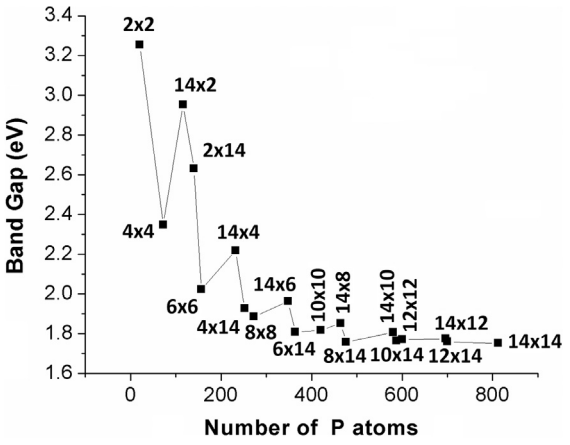

Fig. 6. Evolution of the band gap with number of P atoms and the corresponding R-squared (R^2).

system. The **14** × **n** nanoflakes show constantly lower bandgaps compared to the **m** × **14** ones. The **14** × **n** systems have long zigzag edges, while **m** × **14** have long armchair edges. The difference in E_g between the two types of nanoflakes is probably not related to the different topology of the edges, but to the different number of atoms. The **14** × **n** systems have more P atoms than the corresponding **n** × **14** nanoflakes, resulting in systematically smaller E_g. Therefore, the modification of the size of the nanoflake could be an effective tool for tuning the E_g of the nanoflake.

It is interesting to note the similarity between the evolution of E_g with the shape and size of phosphorene nanoflakes from the one

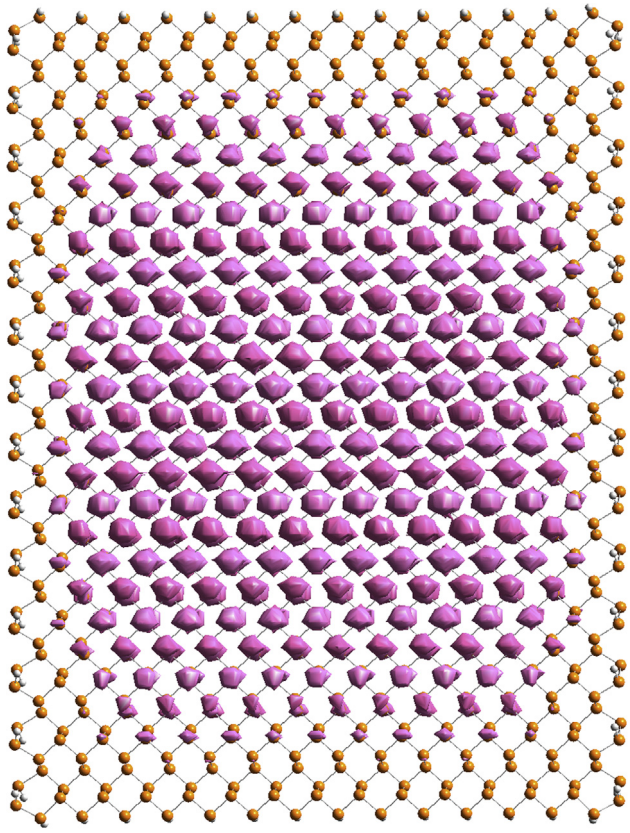

Fig. 7. HOMO for**14** × **14** nanoflake.

side, and the conjugated polymers and GNFs from the other. The drop of the E_g in the GNFs is more rapid with size compared to conjugated polymers [27]. The analogy can be noted when comparing the E_g of **n** × **n** with these of the **14** × **n** or **m** × **14** nanoflakes. As shown in [27], the evolution of E_g for carbon-based conjugated systems depends on the number of connections per atom. The higher the number of connections per atom, the faster the drop of E_g with size. The number of connections per atom in **n** × **n** nanoflakes is greater compared to the **14** × **n** or **m** × **14** nanoflakes, resulting in smaller E_g for **n** × **n** nanoflakes with a similar number of atoms. This is rather unusual, given the puckered structure and lack of conjugation in phosphorene nanoflakes. Moreover, Fig. 5 shows the correlation between E_g of three different types with the reciprocal of the number of atoms (N). As seen from Fig. 5, there is a good correlation between E_g and 1/N, similar to the organic conjugated polymers [28]. This similarity between the phosphorene and

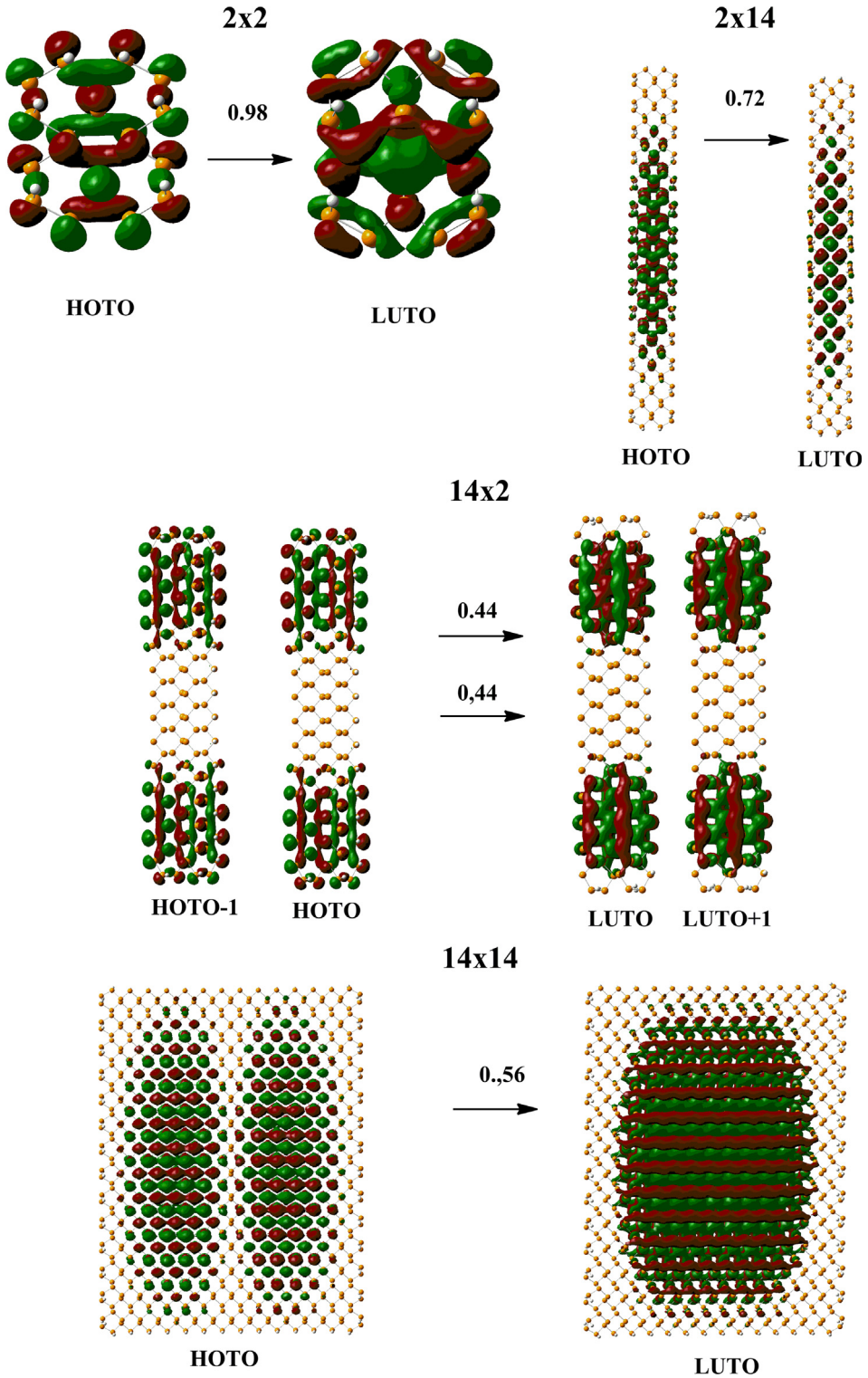

Fig. 8. Highest occupied and lowest unoccupied natural transition orbitals (HOTO and LUTO) for S0 → S1 transitions in selected nanoflakes with associated eigenvalues.

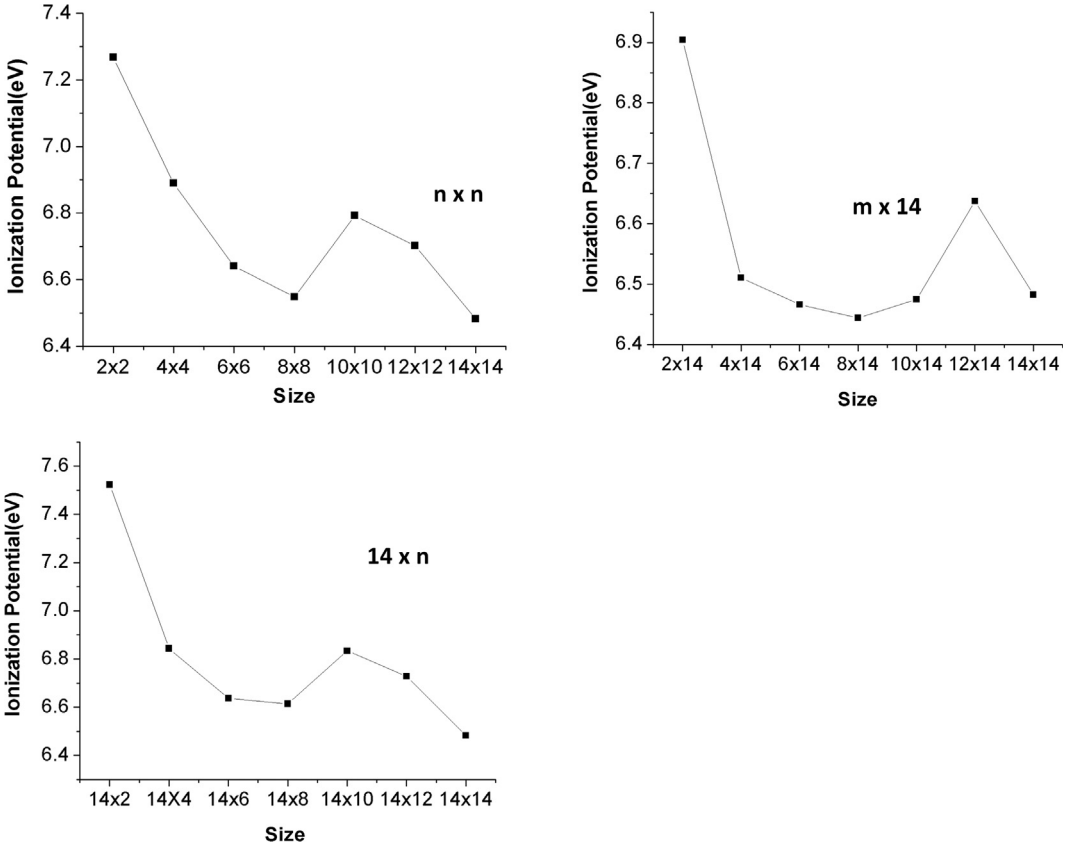

Fig. 9. Evolution of ionization potentials in phosphorene nanoflakes with shape and size.

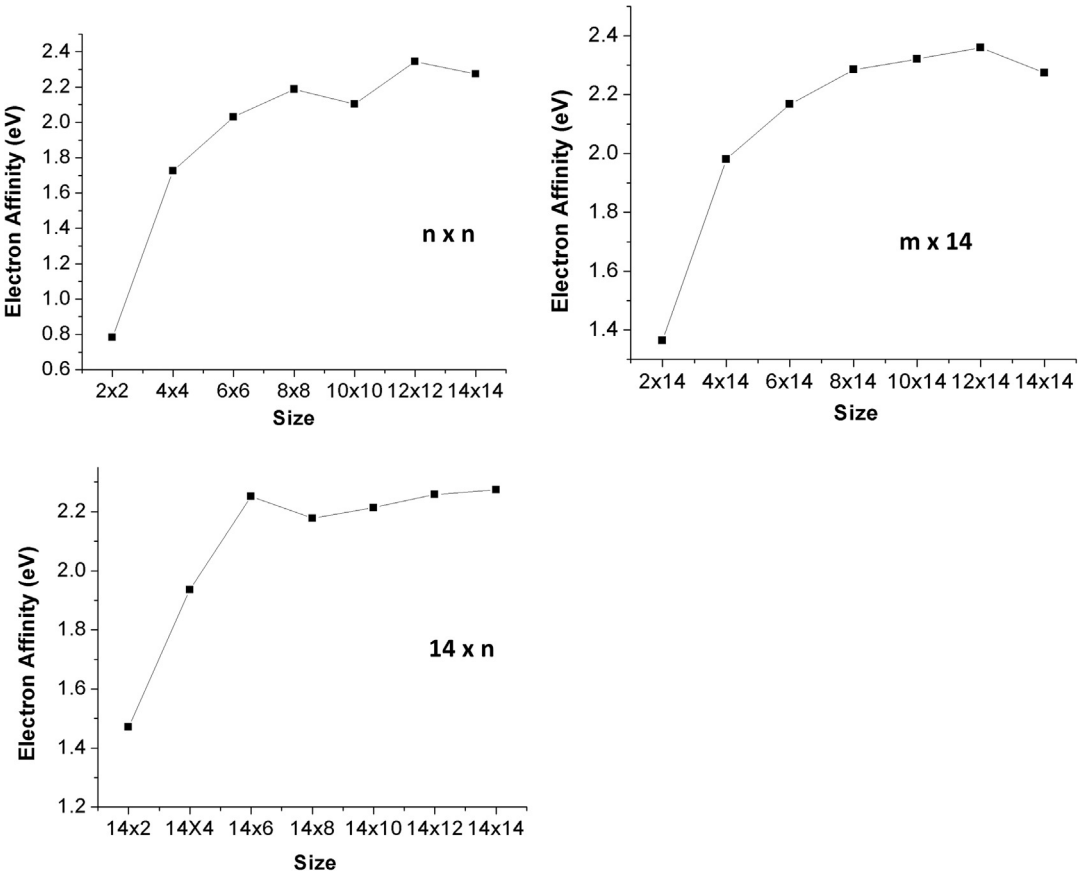

Fig. 10. Evolution of electron affinity in phosphorene nanoflakes with shape and size.

GNFs can be understood by analyzing the molecular orbitals of the phosphorene nanoflakes.

Fig. 7 shows the HOMO of the largest calculated nanoflake, **14** × **14**. The HOMO is composed of $3P_z$ orbitals associated with a lone electron pair of phosphorus atom, which are almost parallel to one another. This arrangement resembles that of $2P_z$ conjugated orbitals in GNFs. The only difference is that the separation between 3Pz orbitals in phosphorene nanoflakes is more than 3 Å, much larger than that of $2P_z$ orbitals in graphene. However $3P_z$ orbitals are also more diffuse, compared to $2P_z$, thus still allowing overlap. This explains the similarity in evolutions of E_g with size between the graphene and phosphorene nanoflakes.

Fig. 8 shows the natural transition orbitals (NTO) for the S0 → S1 transition for selected nanoflakes. The smallest one, **2** × **2**, the biggest one, **14** × **14**, and two rectangular nanoflakes with armchair and zigzag edges, **2** × **14** and **14** × **2**, respectively. The NTO orbitals [29] allow visualization of the electronic transitions when more than two molecular orbitals have important contributions to the excitations. For small **n** × **n** nanoflakes, the S0 → S1 transitions are almost pure HOMO-LUMO excitations. For larger systems, there are more orbitals involved in the S0 → S1 excitation, however, as seen from Fig. 8, no S0 → S1 excitation shows significant charge transfer character, thus validating the data of E_g obtained with the TD-B3LYP functional, which could underestimate the S0 → S1 excitation energies if a significant charge transfer is involved during the excitation. Normally, there is only one or two pairs of NTOs that dominate electronic transitions.

3.2. Charged nanoflakes

Figs. 9 and 10 demonstrate the evolution of the adiabatic ionization potentials (IPs) and the electron affinities (EA) of the nanoflakes with size and shape. There are two important differences between graphene and phosphorene nanoflakes that can immediately be seen. The first and most obvious is that unlike GNFs [26], both the IPs and EAs do not change uniformly with size in phosphorene nanoflakes and the second one is that both IPs and EAs in phosphorene nanoflakes do not change as much with size as for GNFs. The evolution of IPs and EAs for the phosphorene nanoflakes with size is similar to that of GNFs in other aspects. Generally, EAs become larger and IPs become smaller with the size of the nanoflake. To the best of our knowledge, there are no experimental data on the IP and EA of the phosphorene or phosphorene nanoflakes. The theoretically estimated work function for the phosphorene at the GGA level is 5.1 eV [13], notably lower than the almost 6.5 eV IP calculated for the largest **14** × **14** nanoflake. GGA functionals, however, suffer from the self-interaction error, leading to overdelocalization problems [14], with underestimated IPs and overestimated EAs. Unfortunately, the irregular behavior of IPs and EAs with the nanoflake size does not allow for extrapolation for an infinite 2D structure. However, one can observe that even for the largest **14** × **14** nanoflake, the IP is not yet saturated. The shape of the nanoflakes and, especially, the nature or the longest edge (zigzag or armchair) have an important impact on both the IP and EA. Thus, all other things being equal, the **14** × **n** nanoflakes have higher IPs and lower EAs compared to **n** × **n** systems, which is most notable for the smallest members of the series where the shape factor is most important (Fig. 11). Actually, the nanoflake with the highest ionization potential is not the smallest system, **2** × **2**, but **14** × **2**. The nanoflake with the lowest IP is not **14** × **14** but **8** × **14**. A similar situation holds for EAs, where the highest EA is calculated for **2** × **14**, however, the lowest EA, as expected, corresponds to the smallest **2** × **2** nanoflake.

Figs. 12 and 13 show the spin density distribution in polaron cations and anions for selected nanoflakes, respectively, to explain the unusual behavior of the IP and EA with nanoflake size. The spin

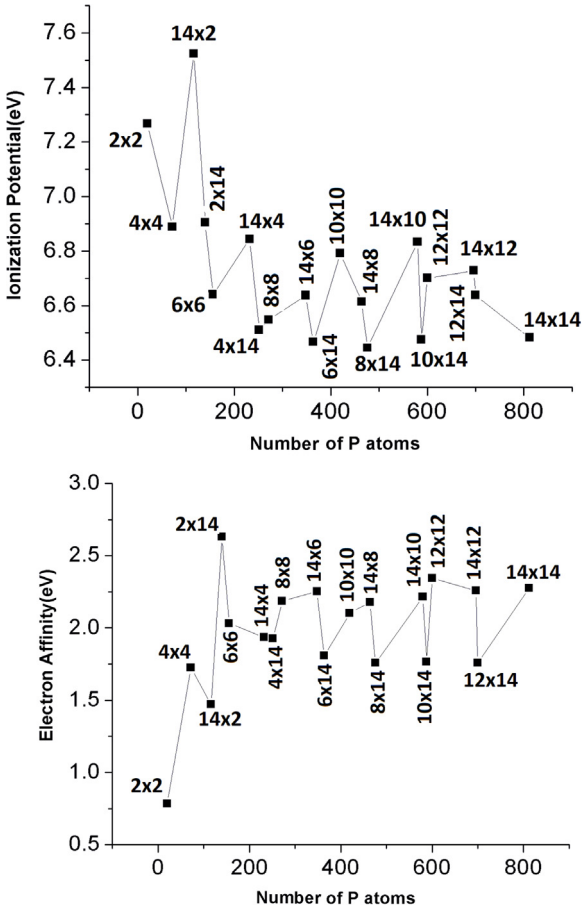

Fig. 11. Evolution of ionization potentials and electron affinity in phosphorene nanoflakes with number of P atoms.

density is associated with the positive charge in polaron cations and with the negative charge in polaron anions, correspondingly. As can be seen from Figs. 9–12, the unusual increase of IP and decease of EA with size is always accompanied by a change in the delocalization pattern of the polaron cations and anions. When the delocalization pattern changes from a single delocalization area to two or from two to four, with the size of a nanoflake, then we observe an increase in IP or a decrease in EA. The explanation of this phenomena is rather straightforward. Multiple delocalization areas imply stronger electron confinement compared to a single delocalization area and, therefore, an increase of total energies of charged species. The increase of the energy of the charged species leads to the increase of IP or the decrease of EA.

As an example we can compare the IPs of **8** × **8** and **10** × **10**. (Fig. 9). The IP of **8** × **8** is 6.5 eV and the IP of **10** × **10** is 6.8 eV. When we look at the delocalization pattern of cation radicals in **8** × **8+** and **10** × **10+** (Fig. 12), we can observe a single delocalization pattern in **8** × **8+** and a double delocalization pattern in **10** × **10+**. A similar situation holds for all cases except for the nanoflakes **14** × **8** and **14** × **10**, where the delocalization pattern of the cation polaron changes from double to quadruple (Fig. 12).

Polaron delocalization causes local geometry distortions in a nanoflake. In the area of polaron anion delocalization, the P-P bond lengths increase to 2.25–2.26 Å, while in the polaron cation delocalization area, the P-P bonds shorten to 2.20–2.21 Å.

Fig. 14 shows the geometries of the **10** × **10+** and **10** × **10**− nanoflakes as an example, where bonds of different lengths have different colors. Thus, the blue colored bonds in the **10** × **10+** correspond to the shortest bonds in the molecules (between 2.20 and 2.21 Å), all other bonds are larger, while the red colored bonds in

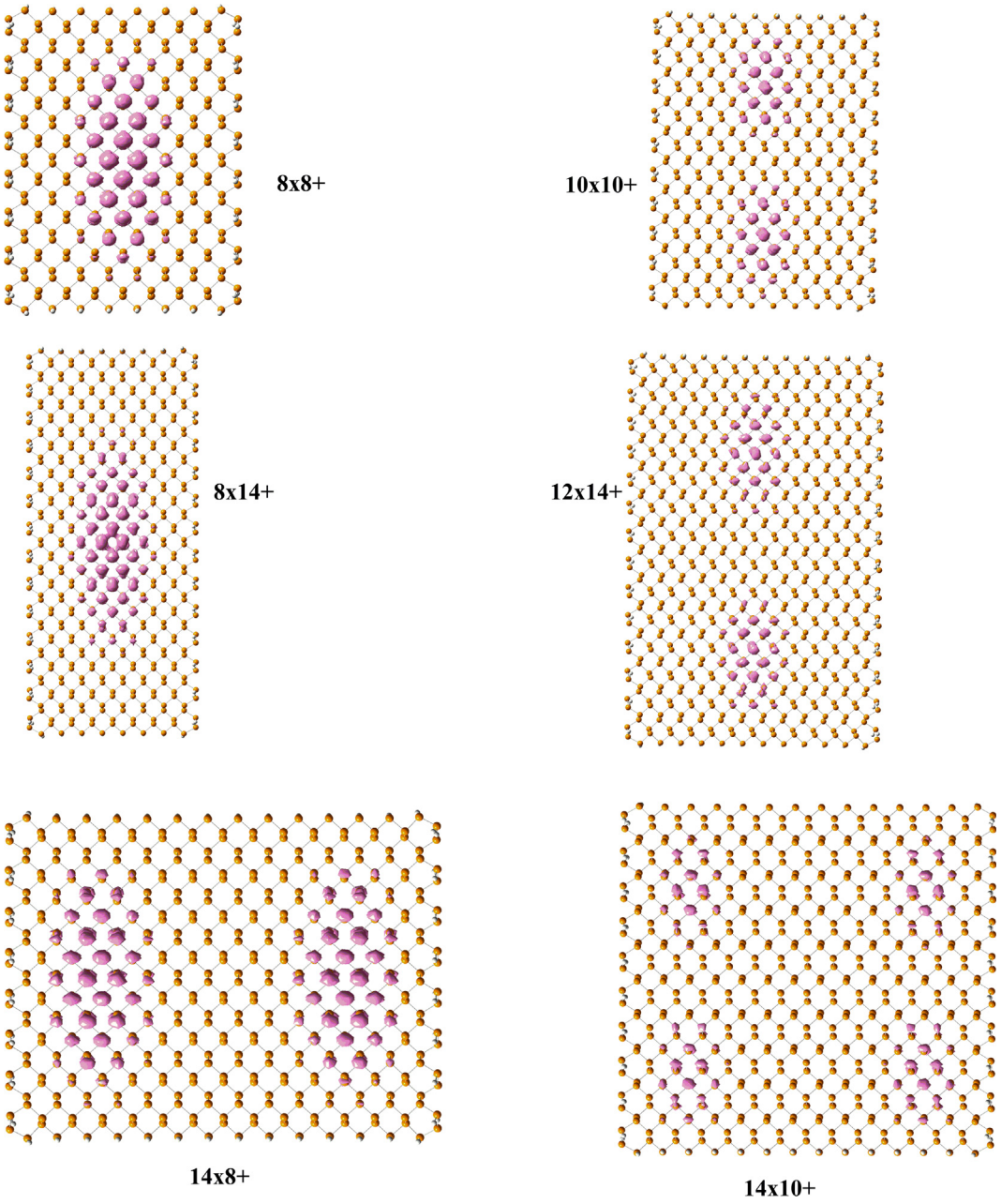

Fig. 12. Spin density distribution in selected polaron cations.

10 × **10** correspond to the longest bonds in the molecule (between 2.25 and 2.26 Å), all other bonds are shorter. In neutral phosphorene, the P-P bond lengths are between 2.224 and 2. 244 Å [19]. When comparing the bond lengths patterns from Fig. 14 with those for the spin density delocalization patterns for the same nanoflakes (Figs. 12 and 13), one can see that there is almost a perfect match between them, demonstrating that the electron detachment or electron attachment causes local geometrical distortion in the nanoflake, which is polaron formation. Electron attachment (formation of a polaron anion) increases electron repulsion, resulting in an increase of the bond lengths in the polaron delocalization area. The electron detachment causes the opposite effect.

Fig. 15 shows calculated reorganization energies for the phosphorene nanoflakes. At first glance, one can observe two important features. The reorganization energies generally decrease with the size of the nanoflake and the hole reorganization energies are smaller than the electron reorganization energies. The low hole reorganization energies estimated theoretically agree very well with the experimentally determined high hole mobility in phosphorene [30], since the low reorganization energies are related with high charge carrier mobility [21–23] Normally, the reorganization energies decrease with size for organic conjugated molecules. Thus, the reorganization energies for triphenylene, coronene and hexa-peri-hexabenzocoronene are 0.18, 0.13 and 0.10 eV, respectively [21–23]. Larger electron reorganization energies compared with hole reorganization energies in the studied phosphorene nanoflakes are due to the different ability of phosphorene to delocalize positive and negative charges. This is especially evident for the **2** × **14** nanoflake, where the difference between λ_- and λ_+ is more than 0.8 eV.

Fig. 16 shows delocalization patterns of the polaron cation and anion for **2** × **14**. As seen, the polaron cation is delocalized almost

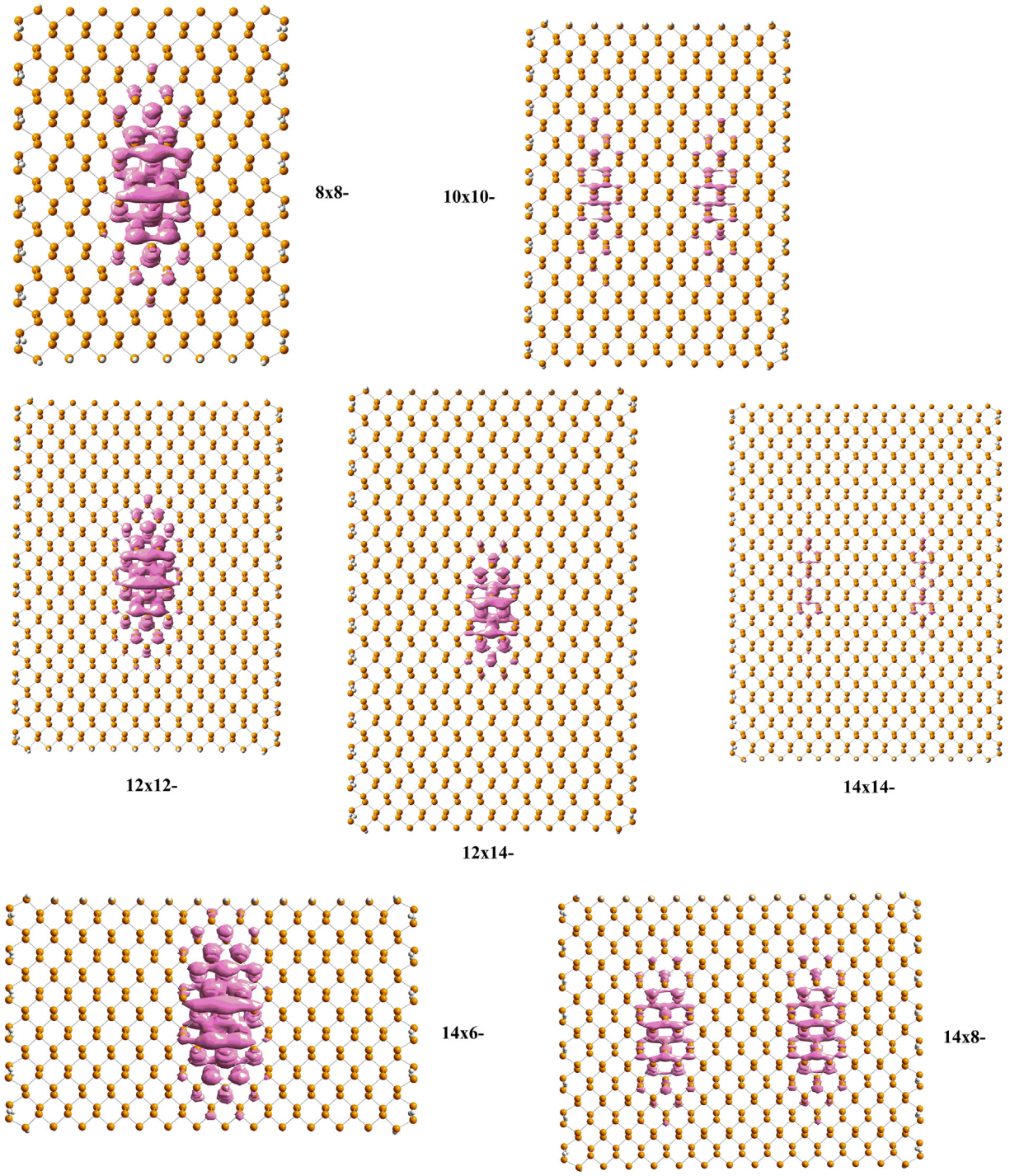

Fig. 13. Spin density distribution in selected polaron anions.

over the entire nanoflake, while the polaron anion is localized in the center of the molecule. This behavior explains the differences between the hole and the electron reorganization energies of the phosphorene nanoflakes.

As seen from Fig. 15, the hole reorganization energies saturate with size much faster than the electron reorganization energies. This is due to much better delocalization of the polaron cations, compared to polaron anion. Actually, for the nanoflakes of the **m** × **14** series, the hole reorganization energy barely depends on the nanoflake size. A very similar situation can be observed for the **n** × **n** series, where λ_+ drops from **2** × **2** to **4** × **4** and then changes very little with size. Both the hole and electron reorganization energies do not change uniformly with size, since the polaron delocalization patterns do not change uniformly with the size of the nanoflakes either.

4. Conclusions

Phosphorene nanoflakes of different sizes and shapes passivated with hydrogen atoms were studied at the hybrid DFT level of theory. The BHandHLYP functional reproduces the experimental bond lengths and valence angles in BP within 0.01 Å and 1°, respectively. All nanoflakes were shown to have singlet ground state and

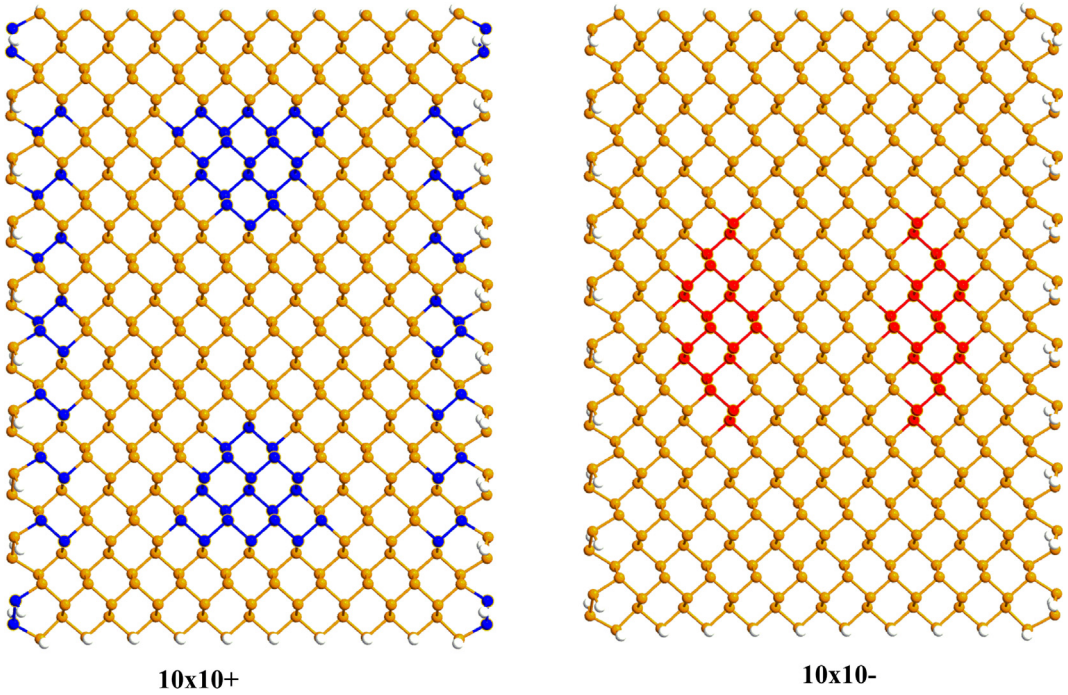

Fig. 14. Molecular geometry deformation in polaron cation and polaron anion of **10** × **10**. Blue color corresponds to the shortest bonds in molecules (2.20–2.21 Å), the red color corresponds to the largest bonds in molecule (2.25–2.26 Å).

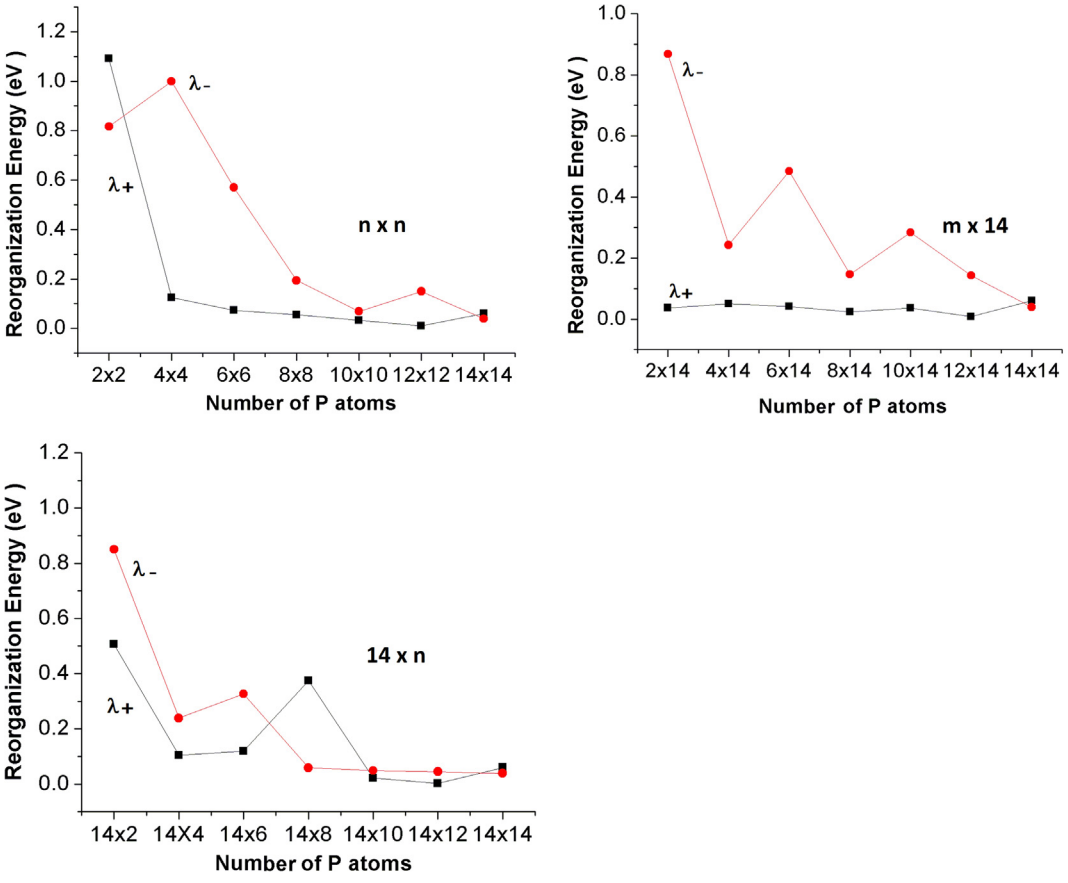

Fig. 15. Evolution of the electron (λ_-) and hole (λ_+) relaxation energies in phosphorene nanoflakes with shape and size.

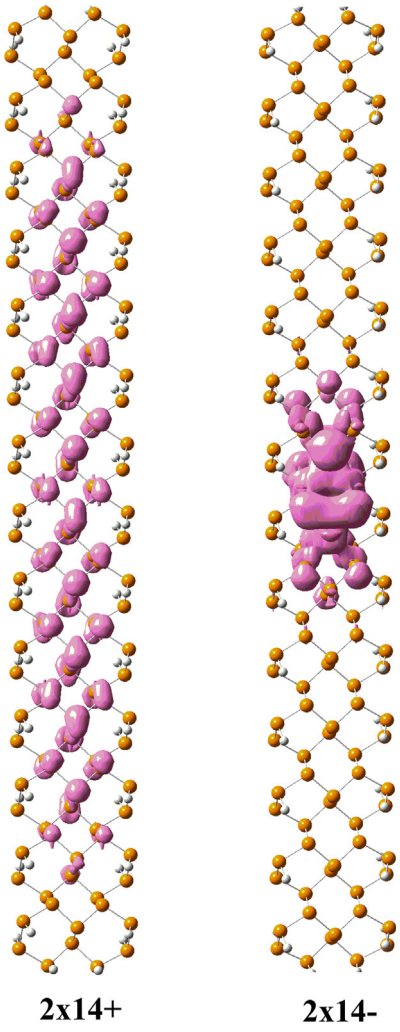

Fig. 16. Difference in the delocalization patterns of cation and anion polarons of **2** × **14** nanoflake.

their E_gs decrease linearly with 1/N, where N is the number of P atoms in the nanoflakes, similar to organic conjugated polymers due to the overlapping of $3P_z$ orbitals of the P atoms. Square nanoflake always have lower E_g than rectangular nanoflakes with the same number of atoms due to larger number of connections per atom. The topology of the nanoflake edges does not seem to affect the E_g.

IPs and EAs tend to decrease with nanoflake size, similar to organic conjugated systems. The change of IPs and EAs with size correlates with the delocalization pattern of polaron cations and anions. The shape and nature of the longest edge (zigzag or armchair) has an important impact on both the IP and EA. Thus, all other things being equal, **14** × **n** nanoflakes have higher IP and lower EA compared to square systems.

Phosphorene nanoflakes show low calculated hole reorganization energies (less than 0.1 eV) in agreement with experimentally observed high hole mobility. Low hole reorganization energies, compared to electron reorganization energies, are related with better delocalization of polaron cations compared to polaron anions.

Acknowledgments

We acknowledge the financial support from CONACyT (Grant 251684) and from supercomputing facilities of National Autonomous University of Mexico.

Appendix A. Supplementary material

Supplementary data associated with this article can be found, in the online version, at https://doi.org/10.1016/j.comptc.2018.03.007.

References

[1] P.W. Bridgman, Two new modifications of phosphorus, J. Am. Chem. Soc. 36 (1914) 1344–1363, https://doi.org/10.1021/ja02184a002.
[2] J.O. Island, G.A. Steele, H.S.J. Van Der Zant, A. Castellanos-Gomez, Environmental instability of few-layer black phosphorus, 2D Mater. 2 (2015) 10.1088/2053-1583/2/1/011002.
[3] A. Castellanos-Gomez, Black phosphorus: narrow gap, wide applications, J. Phys. Chem. Lett. 6 (2015) 4280–4291, https://doi.org/10.1021/acs.jpclett.5b01686.
[4] K.S. Novoselov, A.K. Geim, S.V. Morozov, D. Jiang, Y. Zhang, S. V. Dubonos, I. V. Grigorieva, A.A. Firsov, Electric field effect in atomically thin carbon films, Science (80-.). 306 (2004) 666–669. 10.1126/science.1102896.
[5] R. Fei, L. Yang, Strain-engineering the anisotropic electrical conductance of few-layer black phosphorus, Nano Lett. 14 (2014) 2884–2889, https://doi.org/10.1021/nl500935z.
[6] A.H. Woomer, T.W. Farnsworth, J. Hu, R.A. Wells, C.L. Donley, S.C. Warren, Phosphorene: synthesis scale-up, and quantitative optical spectroscopy, ACS Nano 9 (2015) 8869–8884, https://doi.org/10.1021/acsnano.5b02599.
[7] Y. Xu, B. Yan, H.J. Zhang, J. Wang, G. Xu, P. Tang, W. Duan, S.C. Zhang, Large-gap quantum spin hall insulators in tin films, Phys. Rev. Lett. 111 (2013), https://doi.org/10.1103/PhysRevLett. 111.136804.
[8] J. Xie, M.S. Si, D.Z. Yang, Z.Y. Zhang, D.S. Xue, A theoretical study of blue phosphorene nanoribbons based on first-principles calculations, J. Appl. Phys. 116 (2014), https://doi.org/10.1063/1.4893589.
[9] J. Dai, X.C. Zeng, Structure and stability of two dimensional phosphorene with =O or =NH functionalization, RSC Adv. 4 (2014) 48017–48021, https://doi.org/10.1039/C4RA02850C.
[10] A. Ziletti, A. Carvalho, D.K. Campbell, D.F. Coker, A.H. Castro Neto, Oxygen defects in phosphorene, Phys. Rev. Lett. 114 (2015), https://doi.org/10.1103/PhysRevLett. 114.046801.
[11] W. Hu, L. Lin, C. Yang, J. Dai, J. Yang, Edge-modified phosphorene nanoflake heterojunctions as highly efficient solar cells, Nano Lett. 16 (2016) 1675–1682, https://doi.org/10.1021/acs.nanolett.5b04593.
[12] Y. Cai, G. Zhang, Y.W. Zhang, Electronic properties of phosphorene/graphene and phosphorene/hexagonal boron nitride heterostructures, J. Phys. Chem. C 119 (2015) 13929–13936, https://doi.org/10.1021/acs.jpcc.5b02634.
[13] Y. Cai, G. Zhang, Y.W. Zhang, Layer-dependent band alignment and work function of few-layer phosphorene, Sci. Rep. 4 (2014), https://doi.org/10.1038/srep06677.
[14] R.G. Parr, W. Yang, Density-Functional Theory of Atoms and Molecules, 1989. 10.1002/qua.560470107.
[15] TURBOMOLE V7.2 2017, A development of University of Karlsruhe and Forschungszentrum Karlsruhe GmbH, 1989–2007, TURBOMOLE GmbH, Since 2007, available from http://www.turbomole.com.
[16] S. Grimme, J. Antony, S. Ehrlich, H. Krieg, A consistent and accurate ab initio parametrization of density functional dispersion correction (DFT-D) for the 94 elements H-Pu, J. Chem. Phys. 132 (2010), https://doi.org/10.1063/1.3382344.
[17] A.D. Becke, A new mixing of Hartree-Fock and local density-functional theories, J. Chem. Phys. 98 (1993) 1372–1377, https://doi.org/10.1063/1.464304.
[18] F. Weigend, R. Ahlrichs, Balanced basis sets of split valence, triple zeta valence and quadruple zeta valence quality for H to Rn: design and assessment of accuracy, Phys. Chem. Chem. Phys. 7 (2005) 3297, https://doi.org/10.1039/b508541a.
[19] A. Brown, S. Rundqvist, Refinement of the crystal structure of black phosphorus, Acta Crystallogr. 19 (1965) 684–685, https://doi.org/10.1107/S0365110X65004140.
[20] C. Hättig, F. Weigend, CC2 excitation energy calculations on large molecules using the resolution of the identity approximation, J. Chem. Phys. 113 (2000) 5154–5161, https://doi.org/10.1063/1.1290013.
[21] B.C. Lin, C.P. Cheng, Z.P.M. Lao, Reorganization energies in the transports of holes and electrons in organic amines in organic electroluminescence studied by density functional theory, J. Phys. Chem. A 107 (2003) 5241–5251, https://doi.org/10.1021/jp0304529.
[22] M. Malagoli, J.L. Brédas, Density functional theory study of the geometric structure and energetics of triphenylamine-based hole-transporting molecules, Chem. Phys. Lett. 327 (2000) 13–17, https://doi.org/10.1016/S0009-2614(00)00757-0.
[23] K. Sakanoue, M. Motoda, M. Sugimoto, S. Sakaki, A Molecular orbital study on the hole transport property of organic amine compounds, J. Phys. Chem. A 103 (1999) 5551–5556, https://doi.org/10.1021/jp990206q.
[24] G. Trtaquier, N. Suaud, J.P. Malrieu, Theoretical design of high-spin polycyclic hydrocarbons, Chem. – A Eur. J. 16 (2010) 8762–8772, https://doi.org/10.1002/chem.201000044.
[25] R. Flores, A.E. Torres, S. Fomine, Substituent effect on the spin state of the graphene nanoflakes, RSC Adv. 6 (2016) 64285–64296, https://doi.org/10.1039/C6RA14279F.

[26] A.E. Torres, R. Flores, S. Fomine, A comparative study of one and two dimensional π-conjugated systems, Synth. Met. 213 (2016) 78–87, https://doi.org/10.1016/j.synthmet.2016.01.005.
[27] R. Gutzler, D.F. Perepichka, π-electron conjugation in two dimensions, J. Am. Chem. Soc. 135 (2013) 16585–16594, https://doi.org/10.1021/ja408355p.
[28] J.L. Brédas, R. Silbey, D.S. Boudreaux, R.R. Chance, Chain-length dependence of electronic and electrochemical properties of conjugated systems: polyacetylene, polyphenylene, polythiophene, and polypyrrole, J. Am. Chem. Soc. 105 (1983) 6555–6559, https://doi.org/10.1021/ja00360a004.
[29] R.L. Martin, Natural transition orbitals, J. Chem. Phys. 118 (2003) 4775–4777, https://doi.org/10.1063/1.1558471.
[30] H. Liu, A.T. Neal, Z. Zhu, Z. Luo, X. Xu, D. Tománek, P.D. Ye, Phosphorene: an unexplored 2D semiconductor with a high hole mobility, ACS Nano. 8 (2014) 4033–4041, https://doi.org/10.1021/nn501226z.